JOURNAL OF VIROLOGY, Apr. 1995, p. 2313–2321 Vol. 69, No. 4
0022-538X/95/$04.00+0
Copyright © 1995, American Society for Microbiology

Two Murine Coronavirus Genes Suffice for Viral RNA Synthesis

KYONGMIN HWANG KIM AND SHINJI MAKINO*

Department of Microbiology, The University of Texas at Austin, Austin, Texas 78712-1095

Received 28 July 1994/Accepted 5 January 1995

We identified two mouse hepatitis virus (MHV) genes that suffice for MHV RNA synthesis by using an MHV-JHM-derived defective interfering (DI) RNA, DIssA. DIssA is a naturally occurring self-replicating DI RNA with nearly intact genes 1 and 7. DIssA interferes with most MHV-JHM-specific RNA synthesis, except for synthesis of mRNA 7, which encodes N protein; mRNA 7 synthesis is not inhibited by DIssA. Coinfection of MHV-JHM containing DIssA DI particles and an MHV-A59 RNA$^-$ temperature-sensitive mutant followed by subsequent passage of virus at the permissive temperature resulted in elimination of most of the MHV-JHM helper virus. Analysis of intracellular RNAs at the nonpermissive temperature demonstrated efficient synthesis of DIssA and mRNA 7 but not of the helper virus mRNAs. Oligonucleotide fingerprinting analysis demonstrated that the structure of mRNA 7 was MHV-JHM specific and therefore must have been synthesized from the DIssA template RNA. Sequence analysis revealed that DIssA lacks a slightly heterogeneous sequence, which is found in wild-type MHV from the 3′ one-third of gene 2-1 to the 3′ end of gene 6. Northern (RNA) blot analysis of intracellular RNA species and virus-specific protein analysis confirmed the sequence data. Replication and transcription of another MHV DI RNA were supported in DIssA-replicating cells. Because the products of genes 2 and 2-1 are not essential for MHV replication, we concluded that expression of gene 1 proteins and N protein was sufficient for MHV RNA replication and transcription.

Mouse hepatitis virus (MHV), a coronavirus, is an enveloped virus with a single-stranded, positive-sense RNA genome of approximately 31 kb (22, 40). The 5′ end of the MHV genomic RNA contains a 72- to 77-nucleotide-long leader sequence (18, 47). Downstream of the leader sequence are the MHV-specific genes, each of which is separated by a special short stretch of sequence, the intergenic sequence. MHV-infected cells yield seven major species of virus-specific subgenomic mRNAs (19, 24). The coronavirus mRNAs are structurally polycistronic, yet they appear to yield only monocistronic proteins; the coronavirus mRNAs share 3′ ends in a nested-set structure wherein each mRNA is progressively one gene longer than its 3′-neighboring gene (19, 24), and only the 5′-most gene of each mRNA is translated. These subgenomic mRNAs are named according to their decreasing order of size from 1 to 7 (19, 24). The mRNA body sequences, which start from the intergenic site consensus sequences, are fused with leader sequence at their 5′ ends (15, 18, 35, 47).

The coronavirus gene products that are necessary and sufficient for coronavirus RNA synthesis have not been identified yet. To date, the MHV genome is known to contain eight or nine genes that are encoded by mRNAs 1, 2, 2-1, 3, 4, 5 (for both 5a and 5b), 6, and 7. The 5′-most MHV gene, gene 1, is 22 kb long and most probably encodes viral RNA polymerase and proteases, the activities that are necessary for MHV RNA synthesis (22). Gene 2 encodes the 30 kDa ns2 protein (55), and gene 2-1, the HE gene, encodes the HE protein (44). The gene 2 and 2-1 products are not essential for MHV replication at least in tissue culture, because an MHV mutant with the majority of gene 2 deleted replicates well in tissue culture (43) and some MHVs do not produce HE protein (44). Gene 3 encodes S protein, which is responsible for binding to cellular receptor (8, 52) and for induction of cell fusion (6, 10, 51). The gene 4 product, the ns4 protein, is detected as a 15-kDa protein in MHV-infected cells (46). Gene 5 contains two open reading frames (ORFs); both ORFs 5a and 5b are encoded in a single mRNA, and the downstream ORF, 5b, is translated preferentially in vitro (4, 23, 45). Neither the ns4 protein nor the ORF 5a product, ns5a protein, appears to be necessary for MHV replication in tissue culture, because synthesis of mRNA 4 is not detected in MHV-S-infected cells and the majority of MHV-S 5a ORF is deleted (53). A minor virus protein corresponding to the MHV 5b gene product, ns5b protein, is present as a virus structural protein in infectious bronchitis virus (26), transmissible gastroenteritis virus (11), and MHV (54). Probably this protein is essential for virus replication. Gene 6 encodes M protein, which is believed to be essential for virus assembly. The most 3′ region of the MHV genome, gene 7, encodes the N protein. N protein binds to MHV genomic RNA, forming a helical nucleocapsid (49). Anti-N antibody inhibits MHV RNA replication in vitro (7), indicating that N protein plays an important role in MHV RNA replication. In tissue culture, ns2, HE, ns4, and ns5a proteins are not necessary for MHV replication. Whether the remaining proteins, S, ns5b, and M, are necessary for MHV RNA synthesis is not known.

Serial undiluted passage of MHV-JHM in DBT cells results in generation of defective interfering (DI) RNAs (28, 36) that can be classified into two types. One is a classical type of DI RNA that requires helper virus infection for replication; the structural and packaging properties of the DI RNAs belonging to this type of DI have been described (28, 34, 38). The other DI type includes DIssA, which is nearly genomic in size (28), replicates by itself in the absence of helper virus infection (33), and is efficiently packaged into MHV particles (36). Almost all MHV mRNA synthesis is strongly inhibited in DIssA-replicating cells, whereas synthesis of mRNA 7 and its product, N protein, is not inhibited (28). RNase T_1 oligonucleotide fingerprinting analysis of DIssA suggested that gene 1 and gene 7 of DIssA are essentially intact, whereas multiple deletions are present from genes 2 to 6 (28).

In this study, we examined the possibilities that mRNA 7 is

* Corresponding author. Mailing address: Department of Microbiology, The University of Texas at Austin, ESB 304, 24th at Speedway, Austin, TX 78712-1095. Phone: (512) 471-6876. Fax: (512) 471-7088. Electronic mail address: makino@mail.utexas.edu.

synthesized from DIssA template RNA, but not from helper virus template RNA, and that the gene 1 products and N protein are sufficient for the MHV RNA synthesis. Our study demonstrated that these possibilities are, in fact, the case. We discuss the potential application of DIssA for viral assembly experiments.

MATERIALS AND METHODS

Viruses and cells. The MHV-A59 temperature-sensitive (*ts*) mutant LA16 (3, 41), the plaque-cloned MHV-JHM, and virus sample obtained after 19 undiluted passages of original plaque-cloned MHV-JHM (JHM19th) (28) were used. Mouse DBT cells (13) were used for RNA transfection and propagation of viruses.

Radiolabeling of viral RNAs and agarose gel electrophoresis. Virus-specific RNAs in virus-infected cells were labeled with $^{32}P_i$ as previously described (37) and separated by electrophoresis on 1% urea–agarose gels as described previously (28).

Preparation of virus-specific intracellular RNA and Northern (RNA) blotting. Virus-specific RNAs were extracted from virus-infected cells (37). For each sample, 1.5 μg of intracellular RNA was denatured and electrophoresed through a 1% agarose gel containing formaldehyde, and the separated RNA was blotted onto nylon filters (14). The RNA on the filters was hybridized with ^{32}P-labeled probes specific for the various regions of MHV RNA (14).

One-dimensional fingerprinting analysis. The ^{32}P-labeled mRNA 7 eluted from the gel was digested exhaustively with RNase T_1 as described previously (31). After digestion, the sample was loaded onto 10% sequencing gels.

RNA transcription and transfection. Plasmids were linearized by *Xba*I digestion and transcribed in vitro with T7 RNA polymerase as described previously (32). The lipofection procedure used for RNA transfection was described previously (30).

Isolation of clones containing DIssA-specific sequence. For the amplification of a DIssA-related subgenomic RNA, cDNA was first synthesized from intracellular RNA as previously described (34), using as a primer oligonucleotide 1116 (5′-CTGAAACTCTTTTCCCT-3′), which binds to positive-strand MHV mRNA 7 at nucleotides 250 to 267 from the 5′ end of mRNA 7. MHV-specific cDNA was then incubated with oligonucleotide 78 (5′-AGCTTTACGTAC CCTCTCTACTATAAAACTCTTGTAGTTT-3′), which binds to antileader sequence of MHV RNA, in PCR buffer (0.05 M KCl, 0.01 M Tris hydrochloride [pH 8.3], 0.0025 M $MgCl_2$, 0.01% gelatin, 0.17 mM each deoxynucleoside triphosphate, 5 U of *Taq* polymerase [Promega]) at 93°C for 30 s, 37°C for 45 s, and 72°C for 100 s for 25 cycles. DIssA subgenomic RNA-specific reverse transcriptase (RT)-PCR products were examined by Southern blot analysis in which RT-PCR products were separated by agarose gel electrophoresis and hybridized with a probe which corresponds to 1.5 to 1.7 kb from the 3′ end of MHV genomic RNA; this probe hybridizes with all MHV mRNAs. The identified 1.2-kb-long DIssA subgenomic RNA-specific RT-PCR product was eluted from the preparative gel and cloned into TA cloning vector (Invitrogen). Clones containing DIssA-specific sequence were isolated by colony hybridization using the probe that was used for Southern blot analysis. For the amplification of DIssA RNA, cDNA was first synthesized from gel-purified DIssA RNA by using oligonucleotide 1116 as a primer. DIssA-specific cDNA was then incubated with oligonucleotide 10121 (5′-GAAGGGTTGTATGTGTTG-3′), which binds to negative-strand MHV RNA at nucleotides 798 to 815 from the 5′ end of gene 2, in PCR buffer under the PCR conditions described above. The 1.2-kb-long DIssA-specific RT-PCR product was eluted from the preparative gel and cloned into a TA cloning vector. Clones containing DIssA-specific sequences were isolated by colony hybridization using the probe which hybridizes at MHV gene 2-1.

Labeling of intracellular proteins, immunoprecipitation, and SDS-PAGE. MHV-infected cells were treated with actinomycin D at 4 h postinfection (p.i.), and intracellular proteins were labeled with [^{35}S]methinonine at 8.5 h p.i. for 20 min. Cell lysate was prepared as described previously (30). Virus-specific proteins were immunoprecipitated by anti-MHV-JHM serum (28) and analyzed by sodium dodecyl sulfate-polyacrylamide gel electrophoresis (SDS) (PAGE). Immunoprecipitated protein was incubated at 37°C for 1 h in sample buffer, instead of at 100°C for 2 min. This treatment avoided the aggregation of M protein on the top of the gel (49). For the analysis of ns5b protein, labeling of intracellular proteins, preparation of cell lysates, and immunoprecipitation of ns5b protein with anti-ns5b antibody were done as described by Leibowitz et al. (23).

Nucleotide sequence accession number. The nucleotide sequence reported has been deposited with GenBank under accession numbers U19766 and U19933 to U19938.

RESULTS

Strategy for analysis of DIssA-related RNAs. We wanted to determine whether mRNA 7 detected in DIssA RNA-replicating cells was derived from the DIssA template or from helper virus genomic template. We established experimental conditions so that DIssA-derived RNA, but not helper virus-derived RNA, was efficiently synthesized. We did this by substituting the MHV-JHM helper virus in the DIssA-containing sample with an MHV-A59 *ts* mutant that has an RNA^- phenotype. Two parental viruses were used: JHM19th and LA16, which is an MHV-A59 *ts* mutant with an RNA^- phenotype. In JHM19th-infected cells, DIssA, mRNA 7, and the 2.2-kb-long DIssE (28) are synthesized, whereas synthesis of the helper virus-derived mRNAs is strongly inhibited by DIssA (28). DBT cells were infected with either JHM19th or LA16 alone or were coinfected with both virus samples and cultured at 32.5°C, which is the permissive temperature for LA16. After overnight incubation, culture fluid was collected and cell debris was removed by low-speed centrifugation. Virus samples were named passage 0 (P0), and these virus samples were further passaged on DBT cells several times at the permissive temperature. Because MHV-A59 usually grows about 10 times better than MHV-JHM, we expected that LA16 would grow better than MHV-JHM in coinfected cells and that during passage, MHV-JHM would be eliminated from the virus samples. We examined this possibility by titrating virus infectivity by plaque assay at the permissive temperature and at the nonpermissive temperature, 39.5°C (Table 1). For MHV-JHM, the ratio of virus infectivity at 39.5°C to infectivity at 32.5°C was 3.6×10^{-1}, and the passaged JHM19th samples showed similar ratios (Table 1). Ratios of LA16 titers at the permissive and nonpermissive temperatures at different passage levels were within the range of 1.0×10^{-4} to 3.0×10^{-5} (Table 1), demonstrating that LA16 maintained the *ts* phenotype during several passages. Reduction of LA16 infectivity during passage at the permissive temperature was probably due to the generation of LA16-derived DI RNAs (see below). The ratios of the titers of virus samples from coinfected cultures at the permissive and nonpermissive temperatures were similar to those of LA16 and were significantly lower than those of MHV-JHM, indicating that a majority of infectious viruses in these samples had the *ts* phenotype. We could not distinguish MHV-JHM-derived plaques and LA16-derived plaques; the plaque morphologies of the two viruses were very similar. We repeated this plaque

TABLE 1. Infectivities of LA16, JHM, and virus samples from coinfected cells at two different temperatures[a]

Sample	Titer (PFU/0.2 ml)		Ratio of titers, 39.5°C/32.5°C
	39.5°C	32.5°C	
LA16			
P0	3.0×10^2	1.0×10^7	3.0×10^{-5}
P1	5.0×10^2	5.0×10^6	1.0×10^{-4}
P2	1.5×10^2	5.0×10^5	3.0×10^{-4}
P3	ND[b]	5.0×10^4	$>5.0 \times 10^{-4}$
LA16 + JHM19th			
P0	3.3×10^3	4.0×10^6	8.3×10^{-4}
P1	5.0×10^2	3.5×10^5	1.4×10^{-3}
P2	3.3×10^2	5.5×10^5	6.0×10^{-4}
P3	8.6×10^2	5.0×10^5	1.7×10^{-3}
JHM19th	3.5×10^4	8.5×10^4	4.1×10^{-1}
JHM20th	5.0×10^5	1.0×10^6	5.0×10^{-1}
JHM21st	8.5×10^4	9.5×10^4	8.9×10^{-1}
JHM22nd	3.0×10^4	3.9×10^4	7.7×10^{-1}
Wild-type JHM	5.0×10^5	1.4×10^6	3.6×10^{-1}

[a] Viruses were passaged at the permissive temperature (32.5°C), and viral infectivities were examined by plaque assay at 32.5 or 39.5°C.
[b] ND, Not detected.

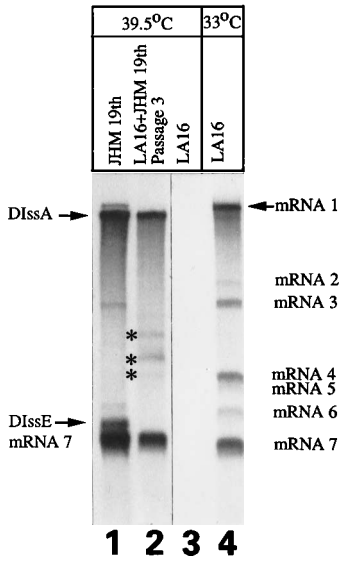

FIG. 1. Urea-agarose gel electrophoresis of MHV-specific intracellular RNA species. DBT cells were infected with JHM19th (lane 1), a P3 virus sample from JHM19th- and LA16-coinfected cells (lane 2), and LA16 (lanes 3 and 4). Viruses were grown at 39.5°C (lanes 1 to 3) or 32.5°C (lane 4), and virus-specific RNA was labeled with $^{32}P_i$ in the presence of actinomycin D. Extracted RNA was electrophoresed on a 1% urea–agarose gel. The three minor bands marked with asterisks (lane 2) were newly synthesized DI RNA species generated during virus passage (see text).

assay experiment twice and obtained similar results. In each virus sample, the difference in the number of plaques from plate to plate varied by less than 20%. This analysis suggested that very little MHV-JHM was present in the virus sample collected from the coinfected culture.

We examined MHV-specific intracellular RNA species of these passaged virus sample at the nonpermissive temperature. DBT cells were infected with the JHM19th alone, LA16 alone, or a P3 sample from coinfected cells. Infected cells were cultured at 39.5 or 32.5°C, and virus-specific RNAs were labeled with $^{32}P_i$ in the presence of actinomycin D. Extracted intracellular virus-specific RNA was electrophoresed on a 1% urea–agarose gel in which mRNA 1 and DIssA are separated easily (28) (Fig. 1). Efficient synthesis of LA16-specific mRNAs was observed at the permissive temperature, whereas LA16-specific mRNA synthesis was not detected at the nonpermissive temperature, confirming that LA16 is an RNA$^-$ *ts* mutant (3, 41). Synthesis of DIssA, DIssE, and mRNA 7 was observed in the cells infected with JHM19th at 39.5°C, demonstrating that synthesis of these RNAs was not temperature sensitive. Synthesis of DIssA and mRNA 7 was clearly apparent in the cells infected with the P3 sample from coinfected cells, whereas synthesis of helper virus mRNAs and DIssE RNA was not detected (Fig. 1, lane 2). This finding was consistent with the plaque assay results; most of MHV-JHM helper virus was eliminated in the P3 sample from the coinfected cells (Table 1). In addition to DIssA and mRNA 7, other minor MHV-specific RNA species were also detected (Fig. 1, lane 2 asterisks); these bands were most likely newly generated DI RNAs (see below). Similar results were obtained when P2 virus samples were examined (data not shown). Helper virus-derived mRNAs, 1 through 6, were not evident at the nonpermissive temperature in the cells infected with the P3 sample from JHM19th- and LA16-coinfected cells; therefore, the mRNA 7 shown in Fig. 1, lane 2, was most likely derived from the DIssA template RNA.

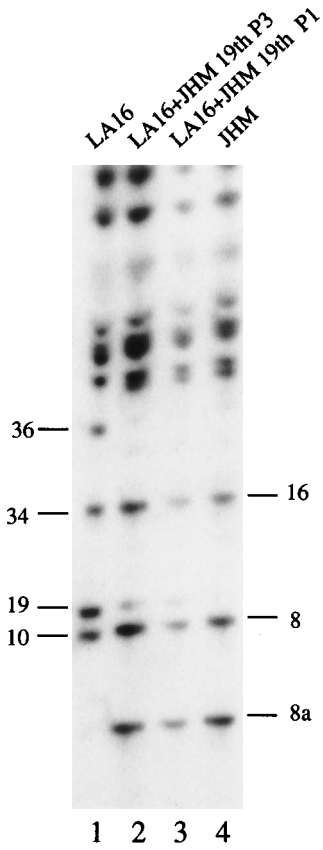

FIG. 2. One-dimensional oligonucleotide fingerprints of mRNA 7 of LA16 (lane 1), of JHM (lane 4), and from cells infected with P1 virus (lane 3) and P3 virus (lane 2) from JHM19th- and LA16-coinfected cells. After separation on urea-agarose gels, ^{32}P-labeled mRNA 7 was extracted from the gels, digested with RNase T_1, and applied to 10% sequencing gels. Electrophoresis was from bottom to top. Numbers show specific oligonucleotides. Oligonucleotides 10 and 8 are leader-specific oligonucleotides of A59 and JHM, respectively (31). Oligonucleotides 19 and 8a are the leader-body fusion oligonucleotides of A59 and JHM, respectively.

It should be noted that DIssA RNA did not complement LA16-specific mRNA synthesis at the nonpermissive temperature (Table 1 and Fig. 1). Probably, DIssA interfered with replication of LA16, because DIssA inhibits MHV-JHM replication (28). We do not know why DIssE disappeared during virus passages; it may be related to the fact that DIssE does not contain a packaging signal (9, 38). DIssE disappeared from virus samples after 24 passages of the original MHV-JHM (27).

Origin of mRNA 7 in the DIssA-replicating cells. We determined whether the mRNA 7 detected in cells infected with P3 sample from JHM19th- and LA16-coinfected cells was actually transcribed from DIssA template RNA. We studied the structure of the mRNA 7 by RNase T_1 one-dimensional oligonucleotide fingerprinting. The experimental RNAs were digested with RNase T_1, and the resultant oligonucleotides were separated on a 10% sequencing gel (Fig. 2); the experimental RNAs included gel-purified ^{32}P-labeled mRNA 7 isolated from cells infected with LA16 alone at 32.5°C, a P1 virus sample from coinfected cells at 39.5°C, a P3 virus sample from coinfected cells at 39.5°C, and MHV-JHM alone at 39.5°C. Fingerprint patterns of LA16 mRNA 7 and of JHM mRNA 7 on the 10% sequencing gel were very similar to those of A59 mRNA 7 and JHM mRNA 7 on the 22% polyacrylamide gels

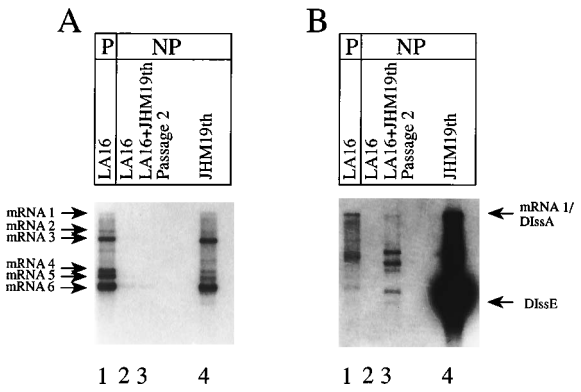

FIG. 3. Northern blot analysis of MHV-specific intracellular RNA species. DBT cells were infected with LA16 (lanes 1 and 2), a P2 virus sample from JHM19th- and LA16-coinfected cells (lane 3), and JHM19th (lane 4). Viruses were grown at 32.5°C (lane 1) or 39.5°C (lanes 2 to 4), and intracellular RNAs were extracted at 9 h p.i., separated by 1% formaldehyde gel electrophoresis, and transferred to a nylon membrane. The probes were prepared by random-primed ^{32}P labeling of MHV-specific cDNA fragments. The probe used for panel A corresponded to genes 5 and 6 of MHV genomic RNA, and the probe for panel B corresponded to 0.47 to 1.5 kb from the 5′-end of MHV-JHM DIssF DI RNA. P, permissive temperature; NP, nonpermissive temperature.

(31); we named the large oligonucleotides as before (31). Oligonucleotides 10 and 8 are the leader-specific oligonucleotides of LA16 and JHM, respectively (31), and oligonucleotides 19 and 8a represent the leader-body fusion sites of LA16 and JHM, respectively (31). The mRNA 7 fingerprint patterns from P1 and P3 samples of coinfected cells were very similar to that of JHM but not to that of LA16. This finding clearly demonstrated that mRNA 7 was indeed synthesized from the MHV-JHM-derived DIssA template RNA. A minor oligonucleotide which comigrated with oligonucleotide 19 was found in the P1 and P3 samples. The leader-body fusion sites of MHV mRNAs are heterogeneous (35), and the 3′ region of DIssA leader sequence is different from that of MHV-JHM (20). Probably this T_1 oligonucleotide represented a heterogeneous leader-body fusion site of the DIssA-derived mRNA 7. Alternatively, oligonucleotide 19 in the P1 and P3 samples may represent a minute amount of revertant LA16 mRNA 7.

Analysis of MHV subgenomic mRNA synthesis, other than mRNA 7, in DIssA-replicating cells. Next we examined which of the other MHV-specific subgenomic mRNAs were synthesized in DIssA-replicating cells. By Northern blot analysis, we determined whether several minor RNA species, detected in cells infected with the P3 sample from JHM19th- and LA16-coinfected cells, were messages (Fig. 1, lane 2, asterisks). We used a probe which corresponds to 0.47 to 1.5 kb from the 5′ end of an MHV-JHM DI RNA, DIssF (28, 38). This probe hybridizes with two regions of the MHV-JHM DI RNA *cis*-acting replication signals (16, 25); it should detect MHV genomic RNA and all of the MHV DI RNAs but not MHV subgenomic mRNAs. As shown in Fig. 3B, this probe not only hybridized with DIssA and DIssE RNAs in the JHM19th-infected cells but also hybridized with DIssA RNA and five minor small-size RNA species in the cells infected with P2 virus from coinfected cells. The apparent difference between the intensities of the DIssA band and the five minor small RNA bands in lane 3 of Fig. 3B and in lane 2 of Fig. 1 reflected the difference between Northern blot analysis and $^{32}P_i$ labeling of intracellular RNAs. Northern blot analysis represents the molar ratio of each RNA species. Labeling with $^{32}P_i$ represents the number of phosphates in any molecule; a larger RNA is expected to be more radioactive than a smaller RNA molecule that has the same number of molecules. This finding demonstrated that the minor RNA bands found in P2 virus-infected cells most probably represented DI RNAs rather than MHV-specific subgenomic RNAs. Several minor bands, which migrated between mRNA 3 to mRNA 6, were found in LA16-infected cells at the permissive temperature. Probably these RNAs also represented LA16-derived DI RNA species.

We looked at MHV-specific mRNAs in DIssA-replicating cells in more depth by using an mRNA 7-exclusive probe. The radiolabeled probe was removed from the nylon membrane used for the experiments shown in Fig. 3B, and the same membrane was rehybridized with a probe which corresponds to part of genes 5 and 6 (1.7 to 3.0 kb from the 3′ end of the MHV genome) (Fig. 3A). This probe should hybridize with mRNAs 1 through 6 and not with mRNA 7. Subgenomic mRNAs were detected both in LA16-infected cells at the permissive temperature and in the JHM19th-infected cells. Only a trace amount of mRNA signal was found in the cells infected with the P2 virus sample from coinfected cells at the nonpermissive temperature; clearly, DIssA did not hybridize with this probe, and MHV subgenomic RNAs containing the sequence corresponding to genes 5 and 6 were not synthesized in DIssA-replicating cells. This result strongly indicated that genes 5 and 6 were missing in DIssA and further confirmed that the smaller RNAs in LA16-infected cells and in P2 virus-infected cells were not MHV subgenomic RNAs but were DI RNAs.

Analysis of the MHV-specific proteins in the DIssA-replicating cells. The Northern blot data indicated that subgenomic mRNAs 3 and 6, which encode the S and M proteins, respectively, were not synthesized in DIssA-replicating cells. To confirm the Northern blot data, we examined S and M protein synthesis in DIssA-replicating cells. DBT cells were infected with viruses, and viral proteins were pulse-labeled with [^{35}S]methionine. At the end of the labeling period, cell lysates were prepared and the MHV-specific proteins were immunoprecipitated with anti-MHV antibody and analyzed by SDS-PAGE (Fig. 4). Minor protein species shown in lanes 8 to 14 of Fig. 4 required longer exposure than proteins in lanes 1 to 7. Synthesis of three major MHV structural proteins, S, N, and M, was evident in the LA16-infected cells at the permissive temperature and in the MHV-JHM-infected cells. Large amounts of N protein and minute amounts of S and M proteins were synthesized in the cells infected with JHM19th (lanes 5 and 12). Synthesis of N protein, but not S and M proteins, was observed in the cells infected with P2 virus from coinfected cells that were incubated at the nonpermissive temperature (lanes 6 and 13); synthesis of S or M protein was not observed even after longer exposure of the gel (lane 13). These data showing that N protein, but not S and M proteins, was synthesized in DIssA-replicating cells were consistent with the data obtained from the intracellular RNA analysis.

We also studied synthesis of MHV ns5b protein in DIssA-replicating cells. Immunoprecipitation by anti-ns5b antibody detected MHV ns5b protein in LA16-infected cells at the permissive temperature but not in MHV-JHM-infected cells or DIssA-replicating cells (data not shown). The amount of ns5b protein in MHV-JHM-infected cells and DIssA-replicating cells was too low to be detected by our experimental conditions.

Primary structure of DIssA. In addition to mRNA 7 subgenomic RNA, DIssA may synthesize small amounts of other DIssA-specific subgenomic RNAs, possibly ns5b-encoding mRNA, and these putative DIssA-specific RNAs might be amplified by RT-PCR. We continued our search for the ns5b protein-encoding region in DIssA by identifying the primary

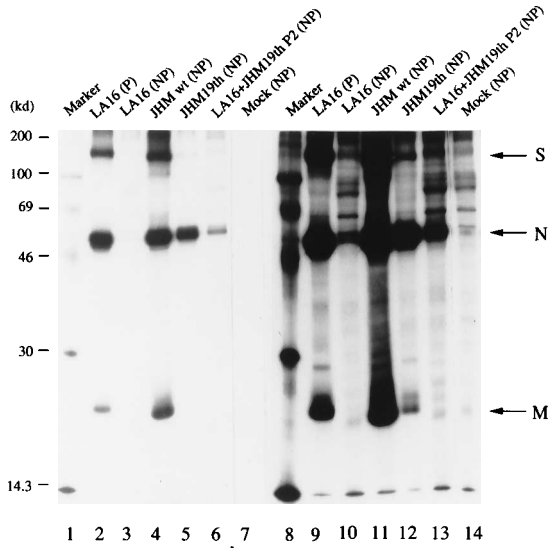

FIG. 4. Analysis of the virus-specific proteins in DIssA-replicating cells. DBT cells were mock infected (lanes 7 and 14) or infected with LA16 (lanes 2, 3, 9, 10), JHM (lanes 4 and 11), JHM19th (lanes 5 and 12), or a P2 sample from LA16- and JHM19th-coinfected cells (lanes 6 and 13). Virus-infected cells were cultured at 32.5°C (lanes 2 and 9) or 39.5°C (lanes 3 to 7 and 10 to 14). At 8.5 h p.i., cultures were pulse-labeled with [^{35}S]methionine, and cytoplasmic lysates were prepared, immunoprecipitated with anti-JHM serum, and electrophoresed on SDS–12% polyacrylamide gels. Positions of MHV S, N, and M proteins are shown on the right. Lanes 8 to 14 represent the overexposures of lanes 1 to 7. Marker represent ^{14}C-labeled protein molecular weight markers. P, permissive temperature; NP, nonpermissive temperature.

structure of DIssA. Sequence analysis of cloned RT-PCR products of putative DIssA-specific subgenomic RNAs should reveal the primary structure of part of DIssA. MHV-specific cDNA was synthesized by using oligonucleotide 1116, which specifically hybridizes 0.25 kb downstream from the intergenic region preceding gene 7. This oligonucleotide should hybridize with all MHV mRNAs and DIssA. The RT-PCR products were synthesized by incubating the cDNA with oligonucleotides 1116 and 78. The latter oligonucleotide hybridizes with the antileader sequence of MHV RNAs. RT-PCR products were then examined by Southern blot analysis with a probe that specifically hybridizes to the 5′ region of gene 7. At both the permissive and nonpermissive temperatures, RT-PCR products corresponding to mRNAs 7, 6, 5, and 4 were observed in the intracellular RNAs from LA16-infected cells, from MHV-JHM-infected cells, and from JHM19th-infected cells (data not shown). In addition, we detected a 1.2-kb-long RT-PCR product in JHM19th-infected cells, whereas we did not find this PCR product in all other samples, indicating that this RT-PCR product was synthesized from a DIssA-specific subgenomic RNA. We isolated this RT-PCR product from a preparative gel and cloned it into a plasmid vector. For isolation of DIssA subgenomic RNA-specific clones by colony hybridization, we used the same probe as for the Southern blot analysis. We identified several clones and completely sequenced two 1.2-kb-long clones, TA23 and TA13.

Sequence analysis revealed that the structure of TA23 was similar to that of MHV-JHM mRNA 2-1 but that it contained a large internal deletion spanning from nucleotide 876 in the transcription initiation site of gene 2-1 (or HE gene) to the 3′ region of gene 6 (Fig. 5). The structure of TA13 was intriguing because of an additional leader sequence that it carried upstream of gene 7; in that cloned PCR product, the 5′-end

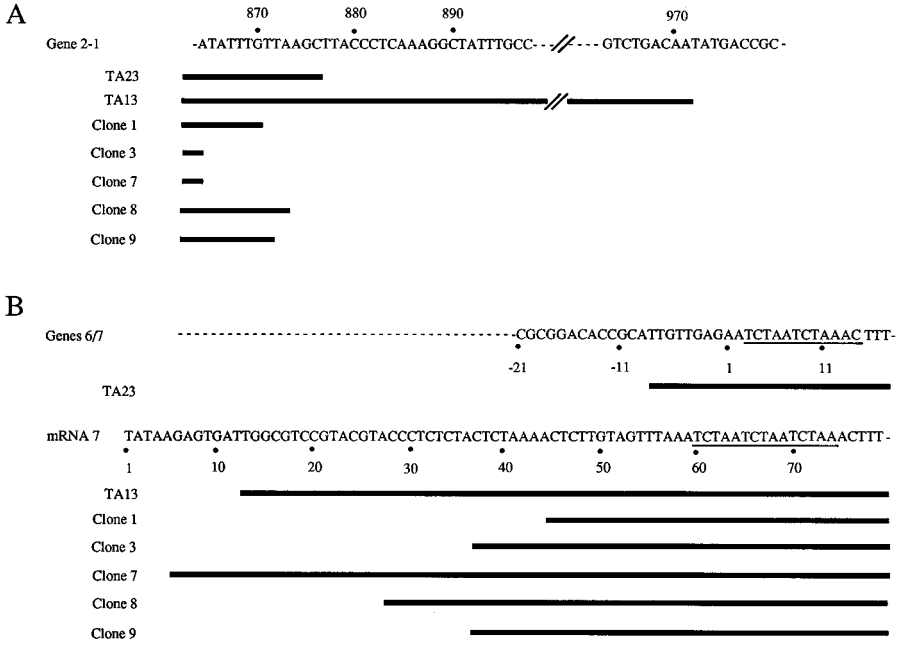

FIG. 5. Schematic representation of the sequence rearrangement sites of cDNA clones of DIssA-specific subgenomic RNA (TA23 and TA13) and cDNA clones of DIssA (clones 1, 3, 7, 8, and 9). (A) The 5′ boundary of the sequence rearrangement site. Bold lines represent the gene 2-1 sequences present in each clone. The sequence of MHV-JHM gene 2-1 (HE gene) was from Shieh et al. (44). Nucleotide numbers of gene 2-1 are from the transcription initiation site of gene 2-1 (44). (B) The 3′ boundary of sequence rearrangement site. Bold lines represent the sequences present in the junction sequence between genes 6 and 7 (for TA23) and those present in the leader sequence of mRNA 7 (for TA13 and other clones). An A nucleotide located two nucleotides upstream of the first two UCUAA repeats is referred to as nucleotide 1 in the junction sequence between genes 6 and 7. For mRNA 7, the most 5′-end nucleotide of mRNA 7 is referred to as nucleotide 1. Intergenic regions are underlined.

region of mRNA 2-1 (972 nucleotides from the transcription initiation site of gene 2-1) was fused to a sequence that resembled mRNA 7 minus 12 nucleotides from the 5′ end. We found no difference in the sequences between the gene 2-1 region of both clones and the published MHV-JHM gene 2-1 (44). The leader-body fusion site of TA23 and TA13 was the same as that of MHV-JHM mRNA 2-1 (44). This sequence analysis suggested that TA23 and TA13 represented cloned cDNAs of DIssA-specific subgenomic RNAs. Because coronavirus mRNA forms a 3′-coterminal nested-set structure, the structures of TA23 and TA13 indicated that DIssA lacks all of genes 3, 4, and 5, most of gene 6, and the 3′ one-third of gene 2-1. The structures of TA23 and TA13 also suggested that the DIssA subgenomic RNA that was used as the template for cDNA cloning was a mixture of RNAs of similar sizes and that these subgenomic RNAs were heterogeneous at the sequence rearrangement site. Consequently, we assumed that DIssA was a group of similar-size RNAs, with heterogeneity in the 5′ and 3′ regions of a large internal deletion site. Presumably some DIssA molecules have a structure in which the 5′ two-thirds of gene 2-1 is fused with a mRNA 7 that lacks several 5′-most nucleotides. DIssA-specific subgenomic RNAs probably expressed the N-terminal two-thirds of the HE protein in DIssA-replicating cells, because we observed that a 32 kDa protein, which was immunoprecipitated by anti-MHV-JHM antibody, was translated in vitro from in vitro-synthesized TA23 RNA (data not shown). The size of this protein translated in vitro was similar to its predicted size.

To confirm that DIssA had a large internal deletion spanning from the 5′ two-thirds to just upstream of the N gene, we examined the structure of DIssA by sequencing cloned DIssA-specific RT-PCR products. On the basis of the structures of TA13 and TA23, cDNA was synthesized from gel-purified DIssA RNA, which was isolated from cells infected with P1 virus from JHM19th- and LA16-coinfected cells, by using oligonucleotide 1116. The RT-PCR products were synthesized by incubating the cDNA with oligonucleotide 1116 and oligonucleotide 10121, which specifically hybridizes to the 3′ region of gene 2. We detected a predicted 1.2-kb-long RT-PCR product in the P1-sample-infected cells, whereas we did not find this PCR product in either MHV-JHM-infected cells or in LA16-infected cells (data not shown). Southern blot analysis demonstrated that this 1.2-kb-long RT-PCR product hybridized with a gene 2-1 probe (data not shown). We cloned this RT-PCR product into a plasmid and sequenced five independent 1.2-kb-long clones, clones 1, 3, 7, 8, and 9 (Fig. 5).

The structures of the DIssA-specific clones were consistent with the structures of DIssA subgenomic RNAs; all of the clones had a deletion spanning from the 3′ one-third of gene 2-1, including genes 3 through 6, to the 5′ end of the mRNA 7-like sequence. Each clone had a slightly different sequence rearrangement site. Therefore, the structures of all of the DIssA-specific clones were similar to that of TA13; in each clone, the 5′-end two-thirds of gene 2-1 were fused with an mRNA 7 that lacked some of the 5′-end nucleotides from the leader sequence. Sequence analyses of the cloned cDNAs from the DIssA-specific subgenomic RNA and DIssA demonstrated that genes 3, 4, 5, and 6 were missing in DIssA.

We further confirmed the structure of DIssA by Northern blot analysis by using a probe corresponding to 362 to 670 nucleotides from the 5′ transcription initiation site of gene 2-1. With this probe, as shown in Fig. 6, two major RNAs, mRNA 1 and mRNA 2, were detected in LA16-infected cells at the permissive temperature (lane 4) and in MHV-JHM-infected cells (lane 1). DIssA and three other RNAs, approximately 5.4, 3.4, and 2.6 kb in length, were detected in the cells infected

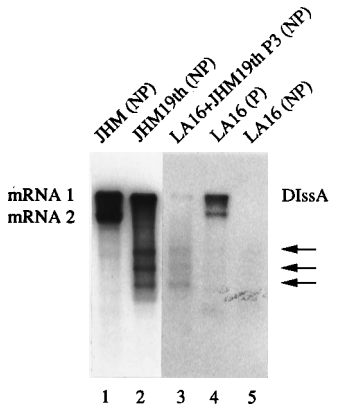

FIG. 6. Northern blot analysis of MHV-specific intracellular RNA species. DBT cells were infected with JHM (lane 1), JHM19th (lane 2), a P3 virus sample from JHM19th- and LA16-coinfected cells (lane 3), and LA16 (lanes 4 and 5). Viruses were grown at 32.5°C (permissive temperature [P]; lane 4) or 39.5°C (nonpermissive temperature [NP]; 1 to 3 and 5), and intracellular RNAs were extracted at 9 h p.i., separated by 1% formaldehyde gel electrophoresis, and transferred to a nylon membrane. The probe was prepared by random-primed ^{32}P labeling of MHV-specific cDNA fragments. The probe correspond to the MHV-JHM HE gene. Three DIssA-specific subgenomic RNAs are shown by arrows.

with JHM19th or with P3 virus from LA16- and JHM19th-coinfected cells. It should be noted that these three additional RNAs were not evident by ^{32}P labeling of DIssA-replicating cells (Fig. 1) or by Northern blot analysis using the 5′-region probe (Fig. 3B), indicating that these were minor RNA species and not DI RNAs. Instead, these three additional RNAs most probably represented the DIssA-specific subgenomic RNAs. The sizes of TA23 and TA13 indicated that they were most likely derived from the smallest, 2.6-kb RNA. On the basis of the sizes of the other two RNAs, the 3.4-kb RNA was probably similar in structure to mRNA 2 but included a large internal deletion like that of TA23 and TA13; probably the largest RNA, the 5.4-kb RNA with a similar deletion, started about 2 kb from the 3′ region of DIssA gene 1. This Northern blot analysis demonstrated that DIssA synthesized three minor RNA species in addition to mRNA 7.

Gene products from DIssA-related RNAs supported replication and transcription of another DI RNA. Our data indicated that the gene 1 products, ns2 protein, part of the HE protein, and the N protein, were expressed in the DIssA-replicating cells and that their expression was sufficient for replication and transcription of these DIssA-related RNAs. Would these gene products support replication and transcription of another DI RNA? We used a DIssF-derived MHV DI cDNA clone, MT 1/24, which contains an inserted intergenic region preceding gene 7 to test this possibility (29). A subgenomic DI RNA is synthesized in MT 1/24-replicating MHV-infected cells (29). MT 1/24 DI RNA was synthesized in vitro and transfected into monolayers of DBT cells which had been infected with LA16 1 h prior to transfection (30). Virus was cultured at 32.5°C, and the P1 virus sample was collected. DBT cells were infected with this P1 virus sample alone, with a P2 virus sample that was collected from LA16- and JHM19th-coinfected cells, or with both the P1 and P2 virus samples. Virus-infected cells were then incubated at the permissive or the nonpermissive temperature. Intracellular RNAs were extracted at 9 h p.i., and equal amounts of intracellular RNAs were examined by Northern blot analysis with a probe corresponding to the 3′ end of MHV genomic RNA (Fig. 7). Lanes 1 to 4 were exposed for the same periods of times; lanes 5 and

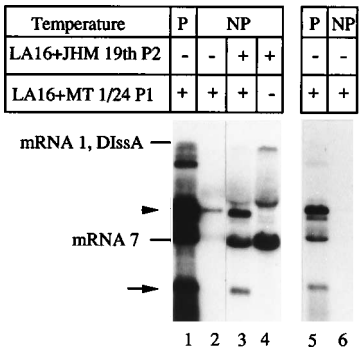

FIG. 7. Northern blot analysis of intracellular RNA species. DBT cells were coinfected with two virus samples, a P2 virus sample from LA16- and JHM19th-coinfected cells and a P1 virus sample from MT 1/24-transfected, LA16-infected cells, and cultured at 32.5°C (permissive temperature [P]; lanes 1 and 5) and 39.5°C (nonpermissive temperature [NP]; lanes 2 to 4 and 6). Intracellular RNA was extracted, and 1.5 μg of cytoplasmic RNA was separated on 1% formaldehyde–agarose gels and transferred to nylon filters. MHV RNA species were detected with a probe corresponding to the 3′ end of genomic RNA. An arrowhead and an arrow represent MT 1/24 genomic DI RNA and subgenomic DI RNA, respectively. Lanes 1 to 4 were exposed for the same length of time. Lanes 5 and 6 are shorter exposure of lanes 1 and 2.

6 represent shortened exposures of lanes 1 and 2, respectively. Synthesis of MT 1/24 genomic DI RNA and subgenomic DI RNA by LA16 was observed at the permissive temperature but not at the nonpermissive temperature (Fig. 7, lanes 1 and 5). We sometimes found that synthesis of LA16-specific mRNAs was somewhat lower in the presence of replicating MT 1/24 than in cells infected with LA16 alone (data not shown and Fig. 7). This was probably caused by homologous interference mediated by MT 1/24 DI RNA. A weak signal which comigrated with genomic MT 1/24 DI RNA (lane 2) may represent a part of the input MT 1/24 DI RNA that was not degraded during incubation. At the nonpermissive temperature, synthesis of DIssA and mRNA 7, but not helper virus-derived mRNA synthesis, was evident in the cells infected with P2 virus from the cells coinfected with LA16 and JHM19th (lane 4). A signal which migrated slightly more slowly than MT 1/24 genomic DI RNA, seen in lane 4, represented 28S rRNA; two minute bands that migrated in approximately the same location as the MT 1/24 genomic DI RNAs were probably other DI RNA species (see above). At the nonpermissive temperature, synthesis of MT 1/24 genomic DI RNA and subgenomic DI RNA was observed in the cells coinfected with the P2 virus sample from LA16- and JHM19th-coinfected cells and the P1 virus sample from MT 1/24-transfected, LA16-infected cells (lane 3). Synthesis of DIssA-related RNAs, DIssA, and mRNA 7, but not infectious virus-specific RNAs, was demonstrated in this RNA sample. The amount of DIssA and mRNA 7 in lane 3 was lower than that found in lane 4; perhaps this indicated that MT 1/24 interfered with RNA synthesis of DIssA and mRNA 7. This finding demonstrated that MT 1/24 genomic DI RNA and its subgenomic DI RNA were synthesized in cells in which DIssA-related RNAs but not helper virus RNAs could be synthesized.

DISCUSSION

In this study, we virtually eliminated MHV-JHM helper virus from DIssA containing MHV-JHM samples and demonstrated that the ensuing mRNA 7 was MHV-JHM-derived DIssA. Through sequence analysis of cDNAs of subgenomic DIssA RNA and genomic DIssA RNA, we identified a deletion in DIssA that extended from the 3′ one-third of gene 2-1 to the end of gene 6; as a result, DIssA-replicating cells were devoid of the subgenomic RNAs encoding S protein, ns4 protein, ns5b protein, and M protein and were devoid of their proteins. Northern blot analysis suggested that four subgenomic RNAs were synthesized from DIssA; they were mRNA 7 and three RNA species of 5.4, 3.4, and 2.6 kb in length. The 2.6-kb-long RNA probably expressed the N-terminal two-thirds of the HE protein. Enzymatic activities associated with DIssA-replicating cells were sufficient for replication and transcription of a non-self-replicating DI RNA, MT 1/24 DI RNA. The ns2, HE, ns4, and ns5a proteins are not involved in MHV RNA synthesis in tissue culture (43, 44, 53); to that list we added the S, ns5b, and M proteins. We concluded that expression of MHV genes 1 and 7 is sufficient for MHV RNA synthesis and that MHV genes 2, 2-1, 3, 4, 5, and 6 are not needed for MHV RNA synthesis.

The present study and an in vitro MHV RNA replication study (7) indicated that the N protein is necessary for MHV RNA synthesis. In negative-strand RNA animal viruses with envelopes, N protein is a part of the helical nucleocapsid; because the nucleocapsid, not naked RNA, functions as template for RNA synthesis, the N protein is required for RNA synthesis (17). The positive-strand RNA animal viruses containing icosahedral capsid, like picornaviruses (2) and viruses belonging to the alphavirus superfamily, do not require any viral structural protein for RNA synthesis (1, 12). Coronavirus RNA synthesis seems to be distinctly different from syntheses of these other positive-stranded RNA animal viruses, because it most probably requires N protein. However, we do not know how the N protein functions in MHV RNA synthesis. Coronavirus nucleocapsid is not required for initiation of coronavirus RNA synthesis, because coronavirus genomic RNA extracted from purified virions is infectious (21, 42). Possibly a subsequent step in coronavirus RNA synthesis, e.g., genomic RNA replication, may require a nucleocapsid template. Binding of MHV N protein at the leader sequence of MHV genomic RNA and subgenomic RNAs has been reported (48), though the biological significance of this binding is still not clear. How coronavirus N protein functions in coronavirus RNA synthesis is fundamental for the understanding of coronavirus RNA synthesis.

We found that the molar ratios of mRNA 1 to mRNA 7 in the helper virus-infected cells and of DIssA and DIssA-derived mRNA 7 in the DIssA-replicating cells were basically the same (Fig. 1). Also, no significant difference was found between the molar ratios of MT 1/24 genomic RNA to subgenomic RNA in LA16-infected cells and in DIssA-replicating cells (Fig. 7). These data indicated that MHV transcription efficiency was not altered by the expression of the MHV S, ns4, ns5a, ns5b, or M protein. This situation is different from that of influenza virus and vesicular stomatitis virus. In these viruses, M protein inhibits viral RNA transcription in vitro (5, 56).

Plaque assay and intracellular viral RNA analysis demonstrated that DIssA did not complement LA16 RNA synthesis at the nonpermissive temperature (Table 1 and Fig. 1). The *ts* site of LA16 was mapped within gene 1, and complementation occurs when LA16 is coinfected with an MHV *ts* mutant belonging to another complementation group (3). Because DIssA inhibits MHV-JHM helper virus-specific mRNA synthesis (28) (Fig. 1), the lack of complementation of LA16 RNA synthesis by DIssA may have been due to interference of LA16 RNA synthesis by DIssA. One speculated mechanism for homologous interference by non-self-replicating DI particles suggests that the DI RNA competes with the helper virus for the limited amount of helper virus-derived polymerase. Homolo-

gous interference by DIssA is probably different from that of non-self-replicating DI RNAs, because DIssA, which synthesizes all of the proteins that it needs for synthesis of itself and its related RNAs, is unlikely to compete for helper virus-derived polymerase activities. The fact that DIssA supported replication and transcription of MT 1/24, which carries a wild-type intergenic sequence (29) and MHV *cis*-acting RNA replication signals (16, 25), indicated that DIssA-derived proteins can recognize wild-type MHV sequences. The lack of complementation of LA16 RNA synthesis by DIssA was, therefore, probably not due to the lack of recognition of the LA16 sequence by DIssA-derived proteins but may the result of some other event happening prior to RNA synthesis.

Sequence analysis of DIssA and its subgenomic RNA demonstrated that most of the DIssA molecules contained a structure in which the 5′-end two-thirds of mRNA 2-1 was fused with an mRNA 7 that lacked some of the most 5′-end several nucleotides from the leader sequence. This structure was most probably generated by nonhomologous RNA recombination between mRNA 7 and mRNA 1. It is possible that during the elongation of negative-strand RNA on the mRNA 7 template, nascent negative-strand RNA switched its template from mRNA 7 to the gene 2-1 region of mRNA 1. Alternatively, this may have been the result of nonhomologous RNA recombination whereby an elongating mRNA 1 switched from mRNA 1 minus-strand template at gene 2-1 to mRNA 7 minus-strand template. We found that the sequence rearrangement site in each cDNA clone was different. Accumulation of DIssA was not, therefore, the result of amplification of one DIssA molecule that was generated by one nonhomologous RNA recombination event but more likely accumulated as the result of multiple nonhomologous RNA recombination events. Insertion of part of the leader sequence in the internal region of the coronavirus genome has been described both for a human coronavirus, OC43 (39), and for a mutant virus isolated from cells persistently infected with MHV-S (50). DIssA maintained part of gene 2-1 and possibly the next gene upstream, gene 2. Why did DIssA contain sequences which are not necessary for MHV RNA synthesis? Hypothetically, a shorter, self-replicating MHV DI RNA carrying only genes 1 and 7 should replicate more efficiently than DIssA. The "extra baggage" of gene 2 and part of gene 2-1, though not required for replication, can be supposed to afford the DI some other advantage.

DIssA lacks four genes and can support replication and transcription of another DI RNA, suggesting that DIssA may be useful for studying coronavirus replication; this is especially important because a full-length coronavirus cDNA does not yet exist and continues to be a challenge to clone. DIssA should support replication and transcription of another DI RNA that subgenomically expresses S protein, ns5b protein, and M protein, and these two DIs should complement; all of the MHV proteins and genomic DI RNAs needed for replication and assembly will then be expressed in the cells, and MHV particles should form and bud. Establishment of such a complementary system, currently in progress in our laboratory, will be invaluable for studying coronavirus assembly mechanisms.

ACKNOWLEDGMENTS

We thank Michael Lai and Stephen Stohlman for LA16 and Julian Leibowitz for anti-ns5b antibody. We thank John Repass and Gwen Giles for excellent technical help.

This work was supported by Public Health Service grants AI29984 and AI32591 from the National Institutes of Health.

REFERENCES

1. **Ahlquist, P., E. G. Strauss, C. M. Rice, J. H. Strauss, J. Haseloff, and D. Zimmern.** 1985. Sindbis virus proteins nsP1 and nsP2 contain homology to nonstructural proteins from several RNA plant viruses. J. Virol. **53:**536–542.
2. **Andino, R., G. E. Riechhof, P. L. Achacoso, and D. Baltimore.** 1993. Poliovirus RNA synthesis utilizes an RNP complex formed around the 5′-end of viral RNA. EMBO J. **12:**3587–3598.
3. **Baric, R. S., K. Fu, M. C. Schaad, and S. A. Stohlman.** 1990. Establishing a genetic recombination map for murine coronavirus strain A59 complementation groups. Virology **177:**646–656.
4. **Budzilowicz, C. J., and S. R. Weiss.** 1987. *In vitro* synthesis of two polypeptides from a nonstructural gene of coronavirus, mouse hepatitis virus strain A59. Virology **157:**509–515.
5. **Caroll, A. R., and R. R. Wagner.** 1979. Role of the membrane (M) protein in endogenous inhibition of in vitro transcription by vesicular stomatitis virus. J. Virol. **29:**134–142.
6. **Collins, A. R., R. L. Knobler, H. Powell, and M. J. Buchmeier.** 1982. Monoclonal antibodies to murine hepatitis virus-4 (strain JHM) define the viral glycoprotein responsible for attachment and cell fusion. Virology **119:**358–371.
7. **Compton, S. R., D. B. Rogers, K. V. Holmes, D. Fertsch, J. Remenick, and J. J. McGowan.** 1987. In vitro replication of mouse hepatitis virus strain A59. J. Virol. **61:**1814–1820.
8. **Dveksler, G. S., M. N. Pensiero, C. B. Cardellicjio, R. K. Williams, G.-S. Jiang, K. V. Holmes, and C. W. Dieffenbach.** 1991. Cloning of the mouse hepatitis virus (MHV) receptor: expression in human and hamster cell lines confers susceptibility to MHV. J. Virol. **65:**6881–6891.
9. **Fosmire, J. A., K. Hwang, and S. Makino.** 1992. Identification and characterization of a coronavirus packaging signal. J. Virol. **66:**3522–3530.
10. **Frana, M. F., J. N. Behnke, S. Sturman, and K. V. Holmes.** 1985. Proteolytic cleavage of the E2 glycoprotein of murine coronavirus: host-dependent differences in proteolytic cleavage and cell fusion. J. Virol. **56:**912–920.
11. **Godet, M., R. L'haridon, J. Vautherot, and H. Laude.** 1992. TGEV corona virus ORF4 encodes a membrane protein that is incorporated into virions. Virology **188:**666–675.
12. **Haseloff, J., P. Goelet, D. Zimmern, P. Ahlquist, R. Dasgupta, and P. Kaesberg.** 1984. Striking similarities in amino acid sequence among nonstructural proteins encoded by RNA viruses that have dissimilar genomic organization. Proc. Natl. Acad. Sci. USA **81:**4358–4362.
13. **Hirano, N., K. Fujiwara, S. Hino, and M. Matsumoto.** 1974. Replication and plaque formation of mouse hepatitis virus (MHV-2) in mouse cell line DBT culture. Arch. Gesamte Virusforch. **44:**298–302.
14. **Jeong, Y. S., and S. Makino.** 1992. Mechanism of coronavirus transcription: duration of primary transcription initiation activity and effect of subgenomic RNA transcription on RNA replication. J. Virol. **66:**3339–3346.
15. **Joo, M., and S. Makino.** 1992. Mutagenic analysis of the coronavirus intergenic consensus sequence. J. Virol. **66:**6330–6337.
16. **Kim, Y.-N., Y. S. Jeong, and S. Makino.** 1993. Analysis of cis-acting sequences essential for coronavirus defective interfering RNA replication. Virology **197:**53–63.
17. **Kingsbury, D. W.** 1974. The molecular biology of paramyxoviruses. Med. Microbiol. Immunol. (Berlin) **160:**73–84.
18. **Lai, M. M. C., R. S. Baric, P. R. Brayton, and S. A. Stohlman.** 1984. Characterization of leader RNA sequences on the virion and mRNAs of mouse hepatitis virus, a cytoplasmic RNA virus. Proc. Natl. Acad. Sci. USA **81:**3626–3630.
19. **Lai, M. M. C., P. R. Brayton, R. C. Armen, C. D. Patton, C. Pugh, and S. A. Stohlman.** 1981. Mouse hepatitis virus A59: mRNA structure and genetic localization of the sequence divergence from hepatotropic strain MHV-3. J. Virol. **39:**823–834.
20. **Lai, M. M. C., S. Makino, L. H. Soe, C.-K. Shieh, J. G. Keck, and J. O. Fleming.** 1987. Coronavirus: a jumping RNA transcription. Cold Spring Harbor Symp. Quant. Biol. **52:**359–365.
21. **Lamniczi, B.** 1977. Biological properties of avian coronavirus RNA. J. Gen. Virol. **36:**531–533.
22. **Lee, H.-J., C.-K. Shieh, A. E. Gorbalenya, E. V. Eugene, N. La Monica, J. Tuler, A. Bagdzhadzhyan, and M. M. C. Lai.** 1991. The complete sequence (22 kilobases) of murine coronavirus gene 1 encoding the putative proteases and RNA polymerase. Virology **180:**567–582.
23. **Leibowitz, J. L., S. Perlman, G. Weinstock, J. R. DeVries, C. J. Budzilowicz, and S. R. Weiss.** 1988. Detection of a murine coronavirus nonstructural protein encoded in a downstream open reading frame. Virology **164:**156–164.
24. **Leibowitz, J. L., K. C. Wilhelmsen, and C. W. Bond.** 1981. The virus-specific intracellular RNA species of two murine coronaviruses: MHV-A59 and MHV-JHM. Virology **114:**39–51.
25. **Lin, Y.-J., and M. M. C. Lai.** 1993. Deletion mapping of a mouse hepatitis virus defective interfering RNA reveals the requirement of an internal and discontiguous sequence for replication. J. Virol. **67:**6110–6118.
26. **Liu, D. X., and S. C. Inglis.** 1991. Association of the infectious bronchitis virus 3c protein with the virion envelope. Virology **185:**911–917.
27. **Makino, S.** Unpublished data.

28. **Makino, S., N. Fujioka, and K. Fujiwara.** 1985. Structure of the intracellular defective viral RNAs of defective interfering particles of mouse hepatitis virus. J. Virol. **54:**329–336.
29. **Makino, S., and M. Joo.** 1993. Effect of intergenic consensus sequence flanking sequences on coronavirus transcription. J. Virol. **67:**3304–3311.
30. **Makino, S., M. Joo, and J. K. Makino.** 1991. A system for study of coronavirus mRNA synthesis: a regulated, expressed subgenomic defective interfering RNA results from intergenic site insertion. J. Virol. **65:**6031–6041.
31. **Makino, S., J. G. Keck, S. A. Stohlman, and M. M. C. Lai.** 1986. High-frequency RNA recombination of murine coronaviruses. J. Virol. **57:**729–737.
32. **Makino, S., and M. M. C. Lai.** 1989. High-frequency leader sequence switching during coronavirus defective interfering RNA replication. J. Virol. **63:**5285–5292.
33. **Makino, S., C.-K. Shieh, J. G. Keck, and M. M. C. Lai.** 1988. Defective-interfering particles of murine coronavirus: mechanism of synthesis of defective viral RNAs. Virology **163:**104–111.
34. **Makino, S., C.-K. Shieh, L. H. Soe, S. C. Baker, and M. M. C. Lai.** 1988. Primary structure and translation of a defective interfering RNA of murine coronavirus. Virology **166:**550–560.
35. **Makino, S., L. H. Soe, C.-K. Shieh, and M. M. C. Lai.** 1988. Discontinuous transcription generates heterogeneity at the leader fusion sites of coronavirus mRNAs. J. Virol. **62:**3870–3873.
36. **Makino, S., F. Taguchi, and K. Fujiwara.** 1984. Defective interfering particles of mouse hepatitis virus. Virology **133:**9–17.
37. **Makino, S., F. Taguchi, N. Hirano, and K. Fujiwara.** 1984. Analysis of genomic and intracellular viral RNAs of small plaque mutants of mouse hepatitis virus, JHM strain. Virology **139:**138–151.
38. **Makino, S., K. Yokomori, and M. M. C. Lai.** 1990. Analysis of efficiently packaged defective interfering RNAs of murine coronavirus: localization of a possible RNA-packaging signal. J. Virol. **64:**6405–6053.
39. **Mounir, S., and P. J. Talbot.** 1993. Human coronavirus OC43 RNA 4 lacks two open reading frames located downstream of the S gene of bovine coronavirus. Virology **192:**355–360.
40. **Pachuk, C. J., P. J. Bredenbeek, P. W. Zoltick, W. J. M. Spaan, and S. R. Weiss.** 1989. Molecular cloning of the gene encoding the putative polymerase of mouse hepatitis virus, strain A59. Virology **171:**141–148.
41. **Schaad, M. C., S. A. Stohlman, J. Egbert, K. Lum, K. Fu, T. Wei, Jr., and R. S. Baric.** 1990. Genetics of mouse hepatitis virus transcription: identification of cistrons which may function in positive and negative strand RNA synthesis. Virology **177:**634–645.
42. **Schochetman, G., R. H. Stevens, and R. W. Simpson.** 1977. Presence of infectious polyadenylated RNA in the coronavirus avian infectious bronchitis virus. Virology **77:**772–782.
43. **Schwartz, B., E. Routledge, and S. G. Siddell.** 1990. Murine coronavirus nonstructural protein ns2 is not essential for viral replication in transformed cells. J. Virol. **64:**4784–4791.
44. **Shieh, C.-K., H. J. Lee, K. Yokomori, N. La Monica, S. Makino, and M. M. C. Lai.** 1989. Identification of a new transcriptional initiation site and the corresponding functional gene 2b in the murine coronavirus RNA genome. J. Virol. **63:**3729–3736.
45. **Skinner, M. A., D. Ebner, and S. G. Siddell.** 1985. Coronavirus MHV-JHM mRNA 5 has a sequence arrangement which potentially allows translation of a second, downstream open reading frame. J. Gen. Virol. **66:**581–592.
46. **Skinner, M. A., and S. G. Siddell.** 1985. Coding sequence of coronavirus MHV-JHM mRNA 4. J. Gen. Virol. **66:**593–596.
47. **Spaan, W., H. Delius, M. Skinner, J. Armstrong, P. Rottier, S. Smeekens, B. A. M. van der Zeijst, and S. G. Siddell.** 1983. Coronavirus mRNA synthesis involves fusion of non-contiguous sequences. EMBO J. **2:**1939–1944.
48. **Stohlman, S. A., R. S. Baric, G. N. Nelson, L. H. Soe, L. M. Welter, and R. J. Deans.** 1988. Specific interaction between coronavirus leader RNA and nucleocapsid protein. J. Virol. **62:**4288–4295.
49. **Sturman, L. S., K. V. Holmes, and J. Behnke.** 1980. Isolation of coronavirus envelope glycoproteins and interaction with the viral nucleocapsid. J. Virol. **33:**449–462.
50. **Taguchi, F., T. Ikeda, S. Makino, and H. Yoshikura.** 1994. A murine coronavirus MHV-S isolate from persistently infected cells has a leader and two consensus sequences between the M and N genes. Virology **198:**355–359.
51. **Taguchi, F., T. Ikeda, and H. Shida.** 1992. Molecular cloning and expression of a spike protein of neurovirulent murine coronavirus JHMV variant cl-2. J. Gen. Virol. **73:**1065–1072.
52. **Williams, R. K., G.-S. Jiang, and K. V. Holmes.** 1991. Receptor for mouse hepatitis virus in a member of the carcinoembryonic antigen family of glycoproteins. Proc. Natl. Acad. Sci. USA **88:**5533–5536.
53. **Yokomori, K., and M. M. C. Lai.** 1991. Mouse hepatitis virus S sequence reveals that nonstructural proteins ns4 and ns5a are not essential for murine coronavirus replication. J. Virol. **65:**5605–5608.
54. **Yu, X., B. Weizhen, S. R. Weiss, and J. L. Leibowitz.** 1994. Mouse hepatitis virus gene 5b protein is a new virion protein. Virology **202:**1018–1023.
55. **Zoltick, P. W., J. L. Leibowitz, E. Oleszak, and S. R. Weiss.** 1990. Mouse hepatitis virus ORF 2a is expressed in the cytosol of infected mouse fibroblasts. Virology **174:**605–607.
56. **Zvonarjev, A. Y., and Y. Z. Ghendon.** 1980. Influence of membrane (M) protein on influenza A virus transcriptase activity in vitro and its susceptibility to rimantadine. J. Virol. **33:**583–586.